GEM - International Journal on Geomathematics (2023) 14:11
https://doi.org/10.1007/s13137-023-00223-y

ORIGINAL PAPER

Characterizing sedimentary processes in abandoned channel using compositional data analysis and wavelet transform

Abdelrhim Eltijani[1] · **David Molnar**[1] · **Janos Geiger**[1]

Received: 24 October 2022 / Accepted: 10 May 2023 / Published online: 24 May 2023

Abstract

Grain size distribution (GSD) is essential for characterizing the deposition process. However, it is necessary to consider its compositional constraint to comprehend the statistical distribution of size fractions within the sediments. Compositional data analysis (CoDA) and wavelet transform (WT) represent alternative methods beyond traditional approaches, e.g., probability density function (PDF). This paper introduces a quantitative approach for characterizing Quaternary depositional and environmental changes using abandoned channel infill sediments. The proposed approach integrates CoDA and WT to thoroughly comprehend the depositional patterns observed in abandoned channels and the underlying environmental variability. The depositional model constructed based on CoDA showed coarsening-upward sequences, suggesting a periodic connection between the main channel and the oxbow lake. Three scales of cycles consistent with the depositional model constructed using CoDA were identified based on WT: small, medium, and large-scale cycles of processes. The large-scale cycles indicate the main depositional events, while the medium and small scale reflects the variation within and during deposition. CoDA and WT demonstrate excellent potential in characterizing the GSD and interpreting oxbow lakes' deposition and sedimentation processes.

Keywords Sedimentary cycles · Compositional data · Wavelet transform · Abandoned channel · Quaternary

Mathematics Subject Classification 86A32 · 86A60

✉ Abdelrhim Eltijani
abdelrhimee@gmail.com

[1] Department of Geology and Paleontology, University of Szeged, 6722 Szeged, Hungary

1 Introduction

Meandering channels are omnipresent features of the Quaternary fluvial system. Abandoned channels are distinct meandering sub-environments that result from complex channel migration over the floodplain (Shen et al. 2021); they develop through consecutive processes of cutoff initiation, plug bar formation, and channel disconnection (Costigan and Gerken 2016; Sedláček et al. 2019; Ielpi et al. 2021). Therefore, understanding abandoned channels' sedimentary processes can contribute significantly to understanding Quaternary fluvial systems. The infill history of the abandoned channel can be observed in vertical sedimentary succession (Hicks and Evans 2022). The sediments of the abandoned channel contain paleoenvironmental proxies that help interpret the depositional processes (Toonen et al. 2012). The infill record exhibits vertical variations corresponding to interconnected sedimentation mechanisms of distinct ranks. Hence, deciphering sedimentary cycles is necessary to understand the hierarchy and extent of sedimentation controls. Grain size distribution (GSD) is a proxy that provides insights into the transport processes and depositional history of abandoned channels. GSDs of fluvial sediments are generally polymodal, with many overlapping individual grain size populations (Collinson and Lewin 1983; Hooke 1995; Eltijani et al. 2022a) deposited by different processes within the same environment (Sun et al. 2002).

GSDs are quantified commonly using log-normal distribution, probability density function (PDF), and multivariate statistics, e.g., principal component analysis (PCA) and cluster analysis (CA). While log-normal results in identical log-normal distribution coefficients for different polymodal GSDs, as GSDs are regularly not log-normal (Roberson and Weltje 2014), PDF may obscure significant variability in GSD. Although multivariate statistics can solve the variability problems, the compositional constraint of GSD requires a prior mathematical treatment because the sum of percentages of the size fractions of GSD sum 100% making a closed system thus, carrying relative information on the whole distribution (Flood et al. 2015).

To address the constraint of GSD, (Eltijani et al. 2022b) employed compositional data analysis (CoDA) and Euclidean data analysis (EuDA) coupled with PCA and CA to examine GSD of a Quaternary abandoned channel located in the southeast Great Hungarian Plain. In the CoDA approach, the raw GSDs were transformed using the centered log-ratio (clr) transformation. In the EuDA approach, raw GSDs were regarded as Euclidean data, needing no prior transformation. The result was distinct models (i.e., EuDA and CoDA models) that are statistically and sedimentologically plausible; their contributions to the conceptual model were substantially distinct.

Our interest was to construct depositional models with statistical significance and geological interpretability. It is worth noting that the models constructed using CoDA and EuDA approaches were deemed plausible based on the statistical assessment and sedimentologic criteria. Nonetheless, the unique contribution of each approach to the conceptual models led to notable differences in the temporal reconstruction of the depositional models.

Although the CoDA helped elucidate the constraint imposed by GSD, and PCA, CA enabled the consideration of the whole GSD and revealing genetic sequences; a comprehensive insight into the evolution requires a quantitative analysis of the vertical sedimentation pattern (i.e., orders and magnitudes) in spatial and temporal scales.

This involves characterizing cyclicity manifested on various orders of magnitude in response to changes in processes that are evident in GSDs, ranging from laminations to beds of centimeter scale.

Cyclic sedimentation is a pattern where the sedimentary sequences develop regularly and repeatedly (Schwarzacher 2000; Allaby 2020). It can be generated by external factors and changes in provenance, e.g., climate and tectonic activity (allocyclic), or by internal factors triggering redistribution of energy and sediment transport within the system (autocyclic) (Allaby 2020). The latter can be represented by meandering channel processes that eventually form an abandoned channel and further influence its sedimentary infills.

Time series analysis is commonly used to discover a steady pattern in regularly measured datasets for identifying and quantifying processes (Gossel and Laehne 2013). The traditional time series models are dependable when applied to long series with hundreds of unreadily available observations that require significant effort to reduce modeling uncertainty. A conventional approach to extract cyclicity uses Fourier transform (FT). The drawback of the FT is that it captures the frequencies over the whole signal; the analysis window cannot capture features in the signals that are either longer or shorter than the window (Prokoph and Patterson 2004). The wavelet transforms (WT) can address the limitations of the FT by enabling the characterization of shorter time series, multiscale, non-steady processes. WT can simultaneously extract local and temporal information, including periods of cyclic events in spatial and time domains (Saadatinejad et al. 2011). Researchers have widely explored the use of WT to interpret geological data, for instance (Perez-Muñoz et al. 2013; Kadkhodaie and Rezaee 2017; Duesing et al. 2021; Li et al., 2022). The commonly employed wavelet techniques are continuous wavelets transformation (CWT) and discrete wavelets transformation (DWT), and the Morlet family is the most used CWT family in earth science. WT can detect gradual and abrupt changes in GSDs and interpret the associated transport and deposition processes.

This paper presents a statistical methodology for analyzing sedimentary time series using GSD data from a Quaternary abandoned channel in the southeast Great Hungarian Plain (GHP). Our approach utilizes CoDA coupled with principal component analysis (PCA) and cluster analysis (CA) to construct a model with statistical significance and geological interpretability. We showed that the CoDA provides a statistically valid, sedimentologically interpretable depositional model. We also demonstrated the application of WT in quantifying the related patterns of transport and deposition processes. We aimed to construct a stochastic model that provides a suitable mathematical representation of the alluviation history of the abandoned channel throughout the mid-late Holocene in the southeast GHP.

2 Material and methods

The material of this study is a 346-cm-long undisturbed sediment core retrieved from the Tövises bed abandoned channel within the geological and geomorphological system of Pocsaj "gate" and Érmellék region in the southeast GHP (Fig. 1). The methodological framework of the analysis is shown in Fig. 2.

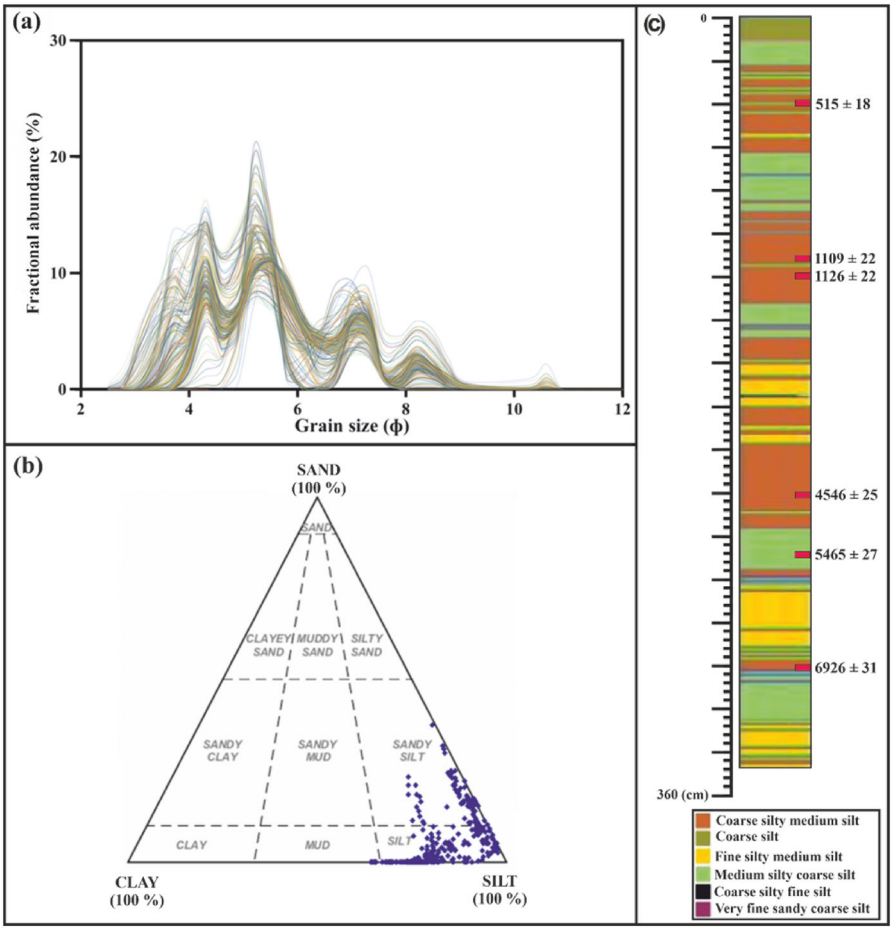

Fig. 1 Grain size distribution (GSD) characteristics of the Tövises bed core. **a** Plot of the GSDs of all samples, illustrating the polymodality of core sediments with six sub modes. **b** Classification of grain size composition in according to the fine ternary plot of (Folk 1954). **c** Lithological and vertical GSDs in the core sediments, the red boxes indicated the chronology samples intervals with their corresponding ^{14}C dates

2.1 Grain size analysis

The laser grain size analysis of the pretreated sediment core samples was conducted at one-cm intervals for 42 grain-size classes from 0.1 to 500 μm for 346 samples (Eltijani and Molnár 2023) using Easysizer20 (OMEC), available at the Department of Geology and Paleontology, University of Szeged, Hungary. The analysis routine and sample treatment are based on (Konert and Vandenberghe 1997) intervals offering 346 samples (Eltijani et al. 2022a) (Fig. 1). Following laboratory measurements, the obtained 42 grain-size classes were segregated into grain-size fractions (clay-fine sand). The grain size nomenclature and classification are based on (Wentworth 1922). Simultaneously, the statistical parameters, i.e., finer percentile (D5), coarser percentile (D95) or (C),

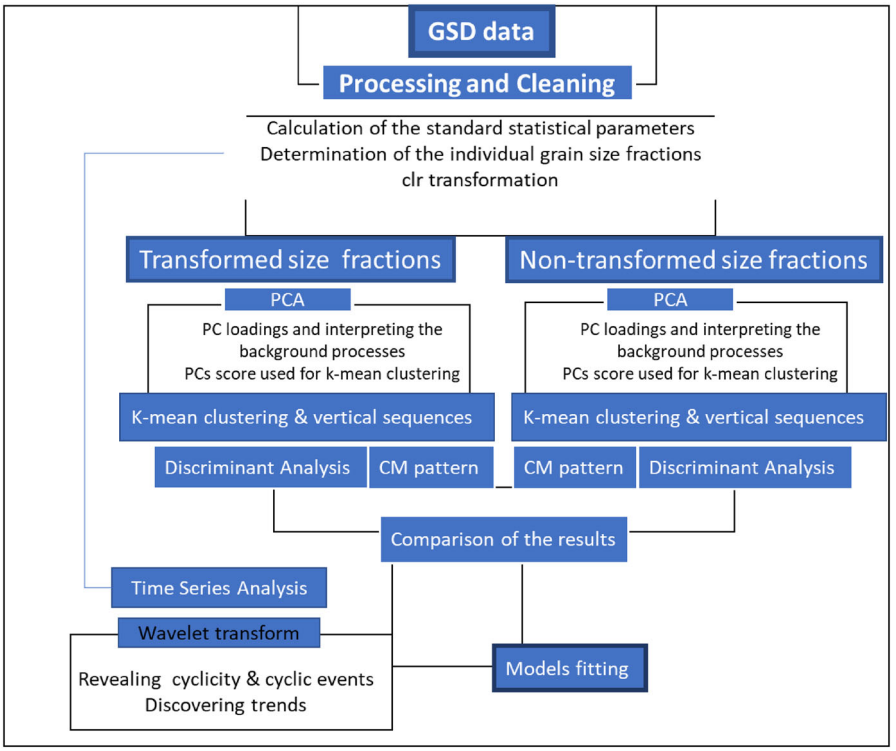

Fig. 2 The methodological framework of the analysis

and the median percentile (Md) or (M), were calculated using the GRADISTAT v. 9.1 of (Blott and Pye 2001). The raw data of this study is presented by (Eltijani and Molnár, 2023).

2.2 ^{14}C dating

The ^{14}C chronology was based on AMS dates from six samples (Eltijani et al. 2022a) analyzed at the International Radiocarbon AMS Competence and Training Center (INTERACT), Debrecen, Hungary. The age-depth model based on Bayesian statistics was constructed using R bacon 2.5.8 in R language version 4.1.3 (Blaauw and Christeny, 2011).

2.3 Rational to CoDA and multivariate statistics

In the previous analysis (Fig. 2), The dataset for the CoDA and EuDA were the statistical parameters of the GSD, D5, D95, Md, and grain size fractions (clay-fine sand). In the case of CoDA, the statistical parameters and grain size fractions were subject to clr-transformation following (Aitchison 1986) conducted in CoDaPack 2.02.21. The

two datasets were subject to PCA; PCA is a pivotal technique for reducing dimensionality (Palazón and Navas 2017; Katra and Yizhaq 2017), allowing the identification of variable groups not visible through other methods. The objective of interpreting PCA results is to identify the geological process "in this case, transportation and sedimentation" processes that underlie the correlations (i.e., loadings) between the principal components (PCs) and the original variables (Szilágyi and Geiger 2012). PCA uses PCs to represent individual transformed observations, which can be interpreted as geological processes. The PC_1 and PC_2 captured most of the total variance, leading to their exclusive consideration for cluster analysis. It is because only those PCs explaining a significant portion of the total variance of the data are studied.

In the hierarchical cluster analysis (HCA) using Ward's method (Ward 1963) with squared Euclidean distance as the similarity coefficient, we employed PC_1 and PC_2 scores as variables. Evaluation of the clustering results is challenging (Pfitzer et al., 2009), and the available internal and external evaluation approaches are much more uncertain (Feldman and Sanger, 2007). As the clustering method relied on these component scores, we postulated that the resultant clusters were indicative of various transport processes within the depositional system. To test this hypothesis, we examined the cluster points in Passega's CM diagram while simultaneously subjecting the statistical validity of the clusters to scrutiny through discriminant analysis (DA).

2.4 Wavelet transformation (WT)

In WT, the primary function is wavelike, referred to as (wavelet) defined by a frequency and a decaying amplitude to zero at the two ends (Duesing et al. 2021). Its time/frequency space is represented in a coordinate system, where the horizontal axis is for the time, and the vertical axis shows the frequency. We focused on the spatial frequency perspective by analyzing depth series and considering t to represent depth. A variable such as $s(t)$ is the signal under consideration (i.e., the sand fraction datasets as a function of the core depth t). CWT decomposes a signal $s(t)$ in terms of some elementary functions $\psi_{a,b}(t)$ derived from the "mother wavelet" $\psi(t)$ by dilation (stretching or compressing) and translation (Addison 2017):

$$\psi_{a,b}(t) = \frac{1}{\sqrt{a}}\psi\left(\frac{t-b}{a}\right) \tag{1}$$

where b represents the position (translation), a (>0) the scale (dilation) of the wavelet, and $\psi_{a,b}(t)$ is the daughter wavelet ($\frac{1}{\sqrt{a}}$) is an energy normalization factor for maintaining the same energy between daughter and mother wavelets (Lau and Hengyi Weng, 1995). The wavelet transform value is the transform of a real signal $s(t)$ with regard to the analyzing wavelet $\psi(t)$ defined as a convolution integral:

$$w_\psi(a,b) = \frac{1}{\sqrt{a}}\int \psi^*\left(\frac{t-b}{a}\right)s(t)dt \tag{2}$$

where a represents the complex conjugate of the mother wavelet $(t)\psi$, a is the location parameter, and b is the scaling dilation parameter. The CWT compares the signal to

shifted and dilated wavelets by comparing the wavelet signals at various scales a and positions b. The result is a function of two variables (Kadkhodaie and Rezaee 2017).

3 Results

3.1 Results of the CoDA modeling

The application of PCA on clr-transformed data yielded two principal components that accounted for 83.22% of the total variance (Fig. 3a). These two principal components represent two distinct depositional processes: the dominant process is indicated by PC1, which explains approximately 60% of the variance, and the less dominant process is indicated by PC2, accounting for around 22% of the variance. As illustrated in Fig. 3b, PC1 exhibits a positive correlation with fine fractions (i.e., clay to medium silts) and a negative correlation with coarser fractions (i.e., medium silt and very fine sand). On the other hand, PC2 shows a positive correlation with the coarse fraction (i.e., medium silt to very fine sand) and a negative correlation with the finer fractions (i.e., clay to fine silt). Thus, the primary process influences the fine fractions, while the second process primarily affects the coarser fractions, indicating the presence of two distinct processes in the oxbow lake.

The PC scores were subjected to cluster analysis, partitioning the sequence into four groups corresponding to specific grain size fractions. The successes of clustering were statistically significant, as indicated by discriminant analysis (DA), with ~ 95% percent correct (Table 1). These groups corresponded to specific depositional processes, as inferred from CM diagram (Fig. 4a). The clusters identified in the analysis were associated with different types of suspension transport: uniform suspensions (SR) and graded suspensions (QR) (Fig. 4b). Three types of QR were described: FG-QR, MG-QR, and CG-QR. These suspensions primarily showed cycles of the coarse CG-QR and MG-QR (Fig. 4a), indicating a periodic connection between the oxbow lake and the main channel (Eltijani et al. 2022b). These suspensions primarily showed cycles of the coarse CG-QR and MG-QR (Fig. 4b), indicating a periodic connection between the oxbow lake and the main channel.

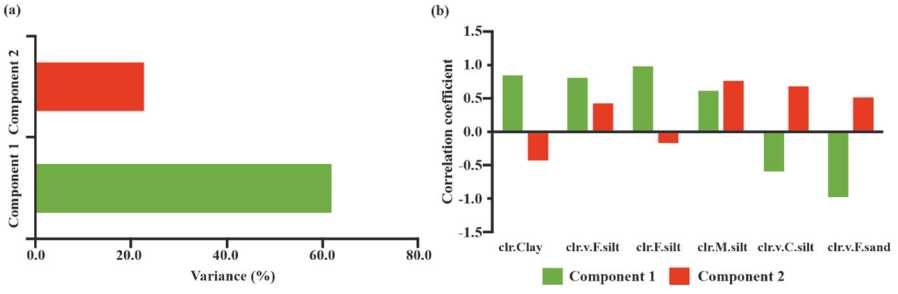

Fig. 3 **a** The scree plot of the variance (%) explained by the first and second principal components (PC_1 and PC_2). **b** Correlation coefficients (loadings) of the PC_1 and PC_2 of the grain size fractions

Table 1 The results of the DA of the CoDA cluster groups

Class	Percent Correct	Cluster 1 p = .1850	Cluster 2 p = .4509	Cluster 3 p = .1503	Cluster 4 p = .2139
Cluster 1	99.1228	113	1	0	0
Cluster 2	100	0	81	0	0
Cluster 3	100	0	0	98	0
Cluster 4	69.8113	0	0	16	37
Total	95.0867	113	82	114	37

3.2 Wavelet transform (WT)

The results of CWT based on the Morlet family applied to sand content of 340 cm intervals are presented in Fig. 5. Due to the finite length of the time series, (edge effects) occur at the two ends of the wavelet spectrum, resulting from stretching the wavelets beyond the sand content series intervals. The information represented by the scalogram is reliable within the cone of influence (Fig. 6). The color patterns of the scalogram indicate the energy magnitude of each wavelet coefficient; the blue patterns correspond to high energy, while the red patterns indicate low energy. The small scales correspond to energy in the input signal at higher frequencies. The medium and large scales correspond to energy in the input signal at medium and lower frequencies.

The CWT for the sand fraction (Fig. 5) shows quasi-periodic small, medium, and large-scale cyclicities. The top of the figure represents detailed, small-scale periods, the middle indicates medium-scale periods, and the bottom represents a smoothed overview of more extended-scale periods. The edge effect is much higher in the bottom than in the middle and upper parts. Thus, this error significantly influences the large-scale periods. Consequently, the wavelets of the entire time series cannot be considered in the case of prolonged periods, only the following intervals: from ~ 100–240, 80–260, 40–290, and 25–320 cm. The sand content series (Fig. 6) shows two large, medium, and three small-scale cycles. Figure 7 clearly shows those depth intervals where these cycles are significant.

The data in Fig. 6 demonstrates that significant cycles of 64 cm occur at the top of the sequence, with less significant cycles at the bottom. The middle of the sequence contains significant cycles of 38 cm, specifically within the range of 140–100 cm and 340–260 cm. Medium scale cycles of 22.5 cm are significant at 180–120 cm and 320–240 cm, while 13 cm cycles are significant at 300–240 cm. The small-scale cycles show the significance for 8 cm cycles at 300–240 cm, while 4.8 cm and 2.5 cm cycles recur significantly throughout the entire sequence. These recurring cycles suggest a predictable pattern in the sequence, which is probably greatly influenced by the autogenic processes of the river system.

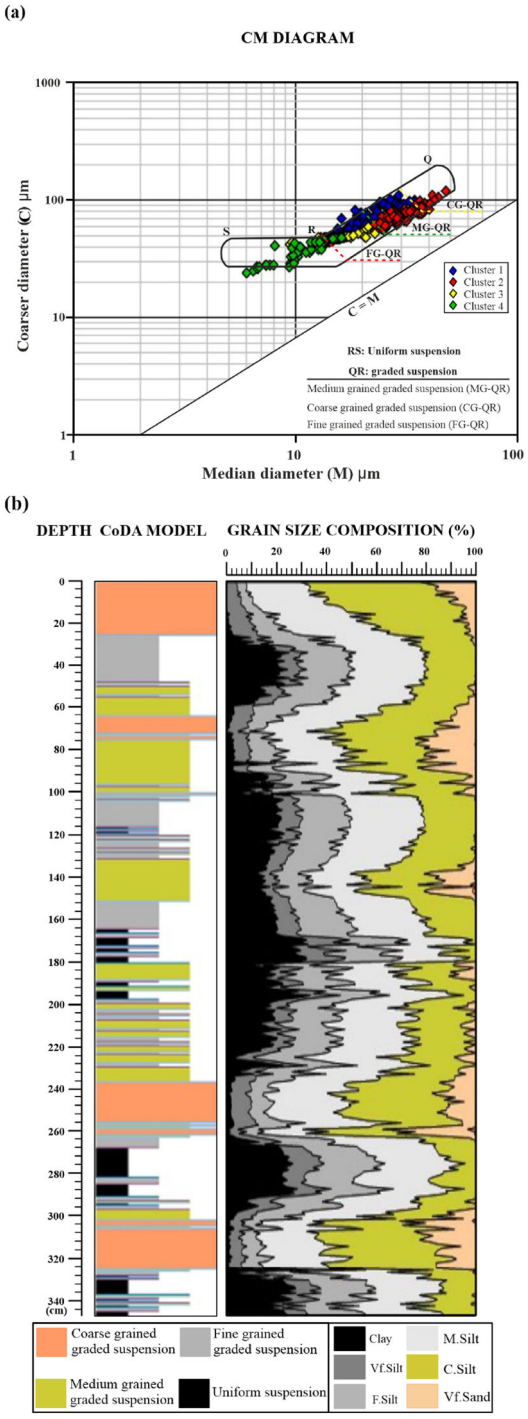

Fig. 4 a The CM diagram illustrating the relations between the clusters groups of the compositional data analysis (CoDA) and their corresponding depositional processes modified after (Passega 1964), the dashed red lines separates the clusters of the uniform suspensions (RS) and the clusters of the graded suspensions (QR) while the green and yellow dashed lines divide the QR into fine, medium and coarse grain graded suspensions. **b** The vertical relations of the depositional processes depositional model constructed based on CoDA as drawn from the CM diagram; modified after Eltijani et al. (2022b)

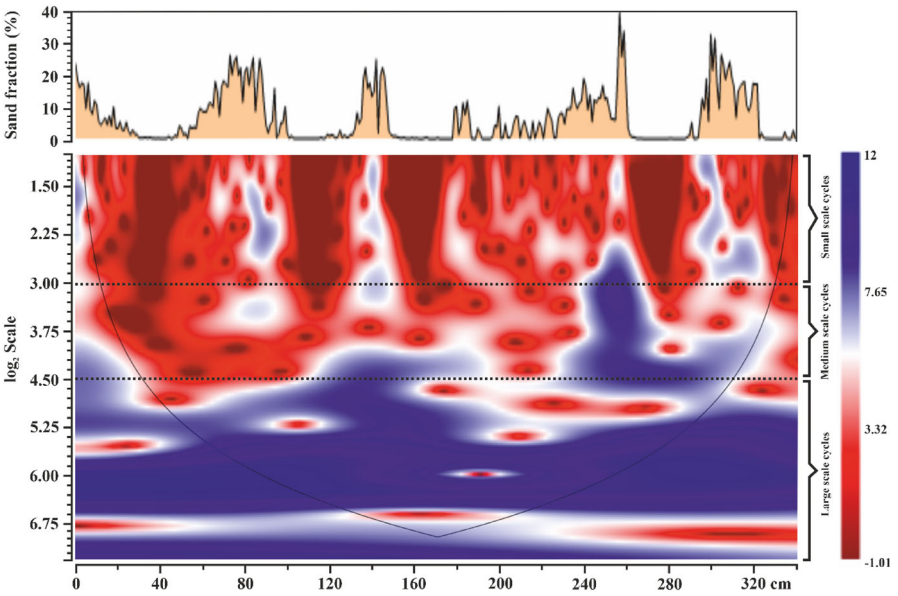

Fig. 5 Represents the analyzed sand content series and its Morlet scalograms representation; the solid line envelope represents the cone of influence. The horizontal dashed lines separate the large, medium and small scales provided by the CWT. In the color scale bar the decreasing infinities indicates the significance of the cycles; the more significant cycles indicate as blue color while less significant cycles indicated as red color. The depth scale panel is shared between scalogram and abundance of sand content

4 Discussion

Employing a CoDA approach in combination with PCA and CA offers the advantage of analyzing the entire GSD, which is not achievable using PDF methods. The fundamental concept is that PDF methodologies entail inherent incongruities besides the lack of sedimentological rationale to support the use of model coefficient parameters for assessing efficacy (Flood et al. 2015). The CoDA model uses an external sedimentological criterion CM diagram, which validates the approach and enables the characterization of two primary suspension processes: RS and QR, with QR further categorized into CG-QR, MG-QR, and FG-QR. This partitioning results from the interaction between overbank depositional processes and abandoned channels' infill sediment (Citterio and Piegay, 2009). Thus, it is likely that CG-QR denotes the stratification resulting from floodplain mechanisms and subsequently integrated into suspended sediments or bedload sediments conveyed by the flood channel. These two alternatives imply the occurrence of high-magnitude flow events.

Analyzing the sand fraction through WT can identify the intensity and the recurrence degree of these transport depositional events and processes. The large-scale cycles depict the general trend of the sedimentation processes and environmental conditions. In contrast, the medium-scale (i.e., intense ~ 22.4, 10, and 8 cm cycles between circa 7 and 6 ka yrs BP and weaker ~ 10 and 8 cm cycles between circa 4–2 ka yrs BP) (Fig. 8a) and small-scale cycles (i.e., ~ 4.5 and 2.8 cm at the bottom of the sequence

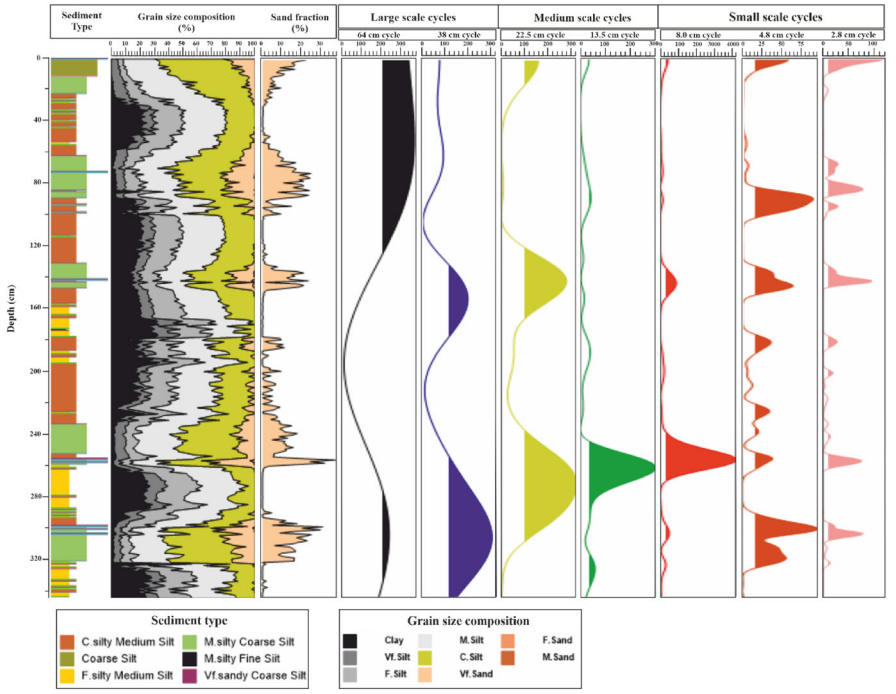

Fig. 6 Representation of the analyzed sand content series and the revealed cycles at the small, medium, and large scales. Two significant large scale in the upper middle and bottom sequences, cycles at the small. Two medium scale cycles significant at the bottom and middle of the sequence. Three significant small-scale cycles are present throughout the entire sequence. The depth panel is shared between the graphs

during the circa 8 -7.5 Ka yrs BP and ~ 4.8 cm at the top of the sequence between circa 2.5–2 ka yrs BP) (Fig. 8b) may reflect the local variability of the transport agent. The background-graded sedimentary sequences are commonly deposited during short-lived events (Hiscott 2003), probably during flooding. These cycles are characterized by upward, downward decreasing, and fluctuation in the sand content (Fig. 7). The upward decrease in the sand content indicates the upward declining energy of the deposition. During this period, turbulence dominates the bottom with a progressive decrease in the energy for all sediment fractions (Hiscott 1994). The upward increase of sand content indicates the upward increase in the available energy during the depositional event. This trend may result from the grain-to-grain collisions caused by the shearing of the overriding bottom current or by the downward percolation of the finer sediments between the coarser grains (Bagnold, 1956). The cycles where variations in sand content repetition show stratified or laminated depositional sequences indicating a recurring short-year flood event.

Comparing these results with the CoDA model (Eltinaji, 2022a and 2022b), the small-scale cycles (Fig. 8b) correspond to CG-QR and MG-QR in the CoDA model indicating cyclic deposition as QR through the active channel or during the overbank flow. The possibility of deposition during a flood is supported by the correlation

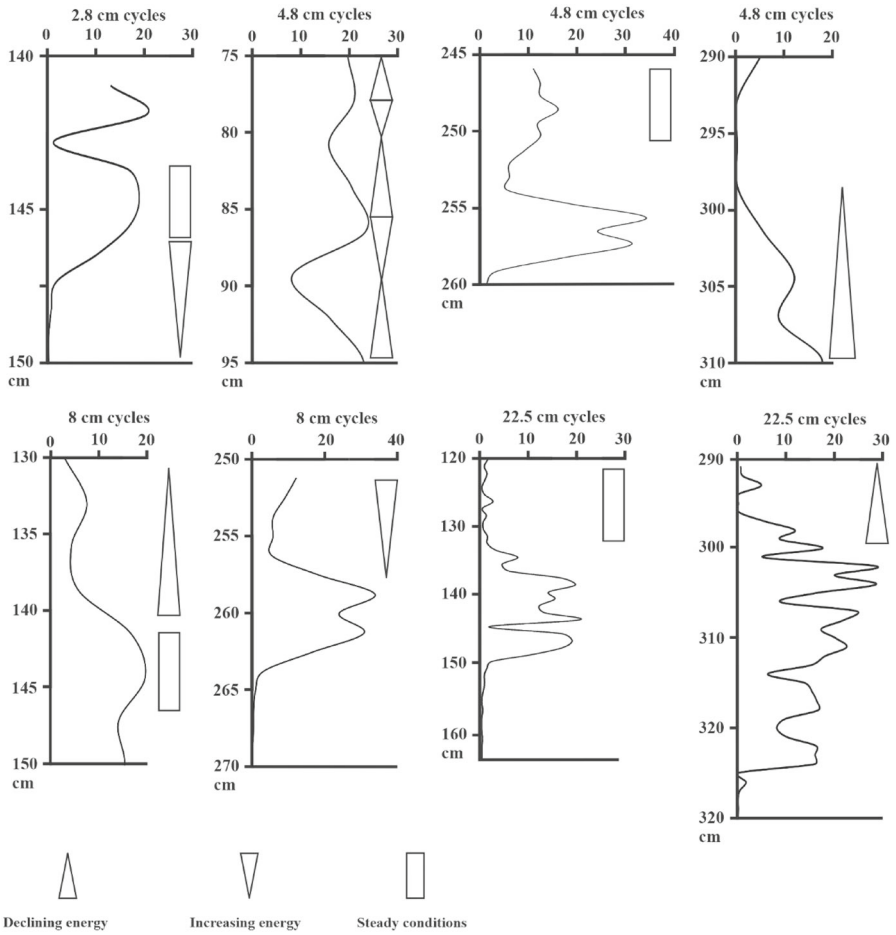

Fig. 7 Represents the medium and small-scale cycles of sand content based on average power spectrum and significance depth intervals with their vertical styles indicating different depositional energy scenarios: coarsening upward cycles (increasing energy), fining upward cycles (declining energy) and intervals where no significant sand content variations (steady energy conditions)

with overbank (OB) units in the Endmember (EMM) model (Fig. 8a, b) (Eltijani et al. 2022a). As the analyzed time series is a CG-QR and MG-QR, the deciphered cycles represent peak depositional energy. The hydraulic settling of the size fractions within QR (in this case CG-QR, MG-QR, and FG-QR) is controlled by a similar process that is partially independent (Passega 1964); two types of currents, competent and incompetent, support the coarser suspension particles. As the competent current velocity is reduced gradually, the coarse to medium silt is deposited with a small amount of clay.

Previous studies have utilized the WT to quantify cyclic sedimentation patterns in different contexts (Rivera et al. 2004; Prokoph and Patterson 2004; Tarar et al. 2018; Wren et al. 2019; Li et al., 2022). For example, the WT was used to study the

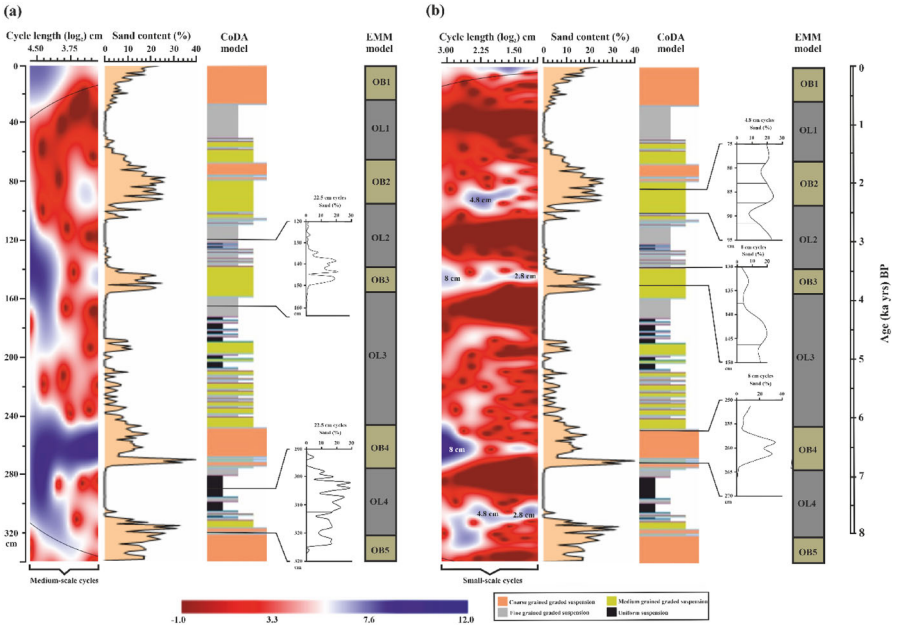

Fig. 8 Represents the medium and small-scale cycles of sand content with their Morlet representation and its scalograms at different scales, average power spectrum, and significance intervals. The color scale bar with decreasing infinities indicates the significance of the cycles the more significant cycles indicated as blue color while less significant cycles indicated as red color. **a** Represent the medium-scale cycles of (~ 4.8 cm), and detailed cyclicity. **b** Represents the small-scale cycles of (~ 4.8 and 2.8 cm). The notions $OB_{1\text{-}5}$ and $OL_{1\text{-}4}$ in the endmember (EMM) model are overbank and oxbow lake intervals respectively. The color scale, legend, depth scale, and the age (before present "BP") bar are shared between the two parts of the figure

cyclicity of point bar sediments using wireline log data as a time series (Perez-Muñoz et al. 2013). The results were similar to previous studies that used the same approach with different time series. However, these results cannot be used as a background for correlation with our model since statistical models are designed to address specific issues and constructed using particular data scales and limits. To our knowledge, this study represents the first quantitative characterization of Quaternary abandoned channel alluviation history using the WT. More quantitative approaches are needed to evaluate changes in sediment transport and deposition associated with changes in autocyclic processes and to assess the abandoned channels infill.

5 Conclusions

This paper aims to provide a quantitative description of the depositional processes based on CoDA and the WT of sand content from the Tövises bed core. The CoDA eliminated the constraint of the GSDs prior to the applications of PCA and CA; PCA and CA characterized the depositional processes based on the whole distribution.

Wavelet analysis provided valuable information for the cyclic alluviation processes of the abandoned channel analyzed from grain size distribution. The study shows that the adequate explanation of the wavelet decomposition and Morlet scalogram helps identify the thickness, depth, and level of significant high-energy depositional events.

- The study revealed that the deposition occurred as uniform and graded suspension loads in multiple stages interrupted with bottom current loads. In the case of CoDA, they corresponded to coarsening-upward sequences, suggesting the periodic sediment flux to the oxbow lake. In contrast, EDA corresponds to fining upward cycles, indicating the permanent weak traction flows with periods of decreasing energy.
- This finding shows excellent potential for using CoDA, coupled with PCA and CA, to interpret the sedimentation processes of abandoned channel sediments with satisfactory statistical significance and geologic interpretations. However, the reliability of this approach should be cross-checked with sedimentological and geological criteria as it cannot consistently deliver a significant result.
- Comparing these cycles with the CoDA model and EMM, the results indicate that cycles can relate to higher energy conditions of different magnitudes. Significant floods occurred at the bottom of the sequence between circa 7–6 ka yrs BP, while moderate flood events can be seen at the top of the sequence during circa 3.5 ka yrs BP; how the middle of the sequence between circa 6–4 ka years BP witnessed week flood events.

Acknowledgements The authors would like to thank all colleagues at the Department of Geology and Paleontology, University of Szeged, for assisting in the technical part of the paper preparation. Special thanks to prof. Pál Sümegi for initiating the project and granting the material subjected to analysis. Thank goes to International Congress on Geomathematics in Earth- & Environmental Sciences and the 22nd Hungarian Geomathematical Congress committee.

Author contributions AE: Conceptualization and methodology, formal analysis, visualization, and original draft writing. JG: Conceptualization methodology and validation, and proofreading. DM: supervision, analysis, project administration, and funding acquisition. The authors applied the SDC approach for the sequence of authors https://doi.org/10.1371/journal.pbio.0050018. All authors have read and agreed to the published version of the manuscript.

Funding The Hungarian Government supported this research, Ministry of Human Capacities (20391-3/2018/FEKUSTRAT).

Data availability All datasets cited and analyzed in this study are available at https://data.mendeley.com/datasets/fgjgv2ymxp/2.

Declarations

Conflict of interest The authors declare that there are no known conflicts of interest associated with this publication, and there has been no significant financial support for this work that could have influenced its outcome.

References

Addison, P.S.: The Illustrated Wavelet Transform Handbook. Biomedical Instrumentation and Technology (2017). https://lccn.loc.gov/2016033578.

Aitchison, J.: The statistical analysis of compositional data. Stat. Anal. Compos. Data **44**(2), 139–177 (1986). https://doi.org/10.1007/978-94-009-4109-0

Allaby, M.: A Dictionary of Geology and Earth Sciences, 5th edn. Oxford University Press, Oxford (2020). https://doi.org/10.1093/acref/9780198839033.001.0001

Blaauw, M., Andrés Christeny, J.: Flexible paleoclimate age-depth models using an autoregressive gamma process. Bayesian Anal. **6**(3), 457–474 (2011). https://doi.org/10.1214/11-BA618

Blott, S.J., Pye, K.: Gradistat: a grain size distribution and statistics package for the analysis of unconsolidated sediments. Earth Surf. Proc. Land. **26**(11), 1237–1248 (2001). https://doi.org/10.1002/esp.261

Citterio, A., Piegay Y, H.: Overbank sedimentation rates in former channel lakes: characterization and control factors. Sedimentology **56**(2), 461–482 (2009). https://doi.org/10.1111/j.1365-3091.2008.00979.x

Collinson, J.D., Lewin, J.: Alluvial cutoofs in wales and the borderlands. Modern Ancient Fluvial Syst. (1983). https://doi.org/10.1016/0037-0738(84)90031-9

Costigan, K.H., Gerken, J.E.: Channel morphology and flow structure of an abandoned channel under varying stages. Water Resour. Res. **52**(7), 5458–5472 (2016). https://doi.org/10.1002/2015WR017601

Duesing, W., Berner, N., Deino, A.L., Verena Foerster, K., Kraemer, H., Marwan, N., Trauth, M.H.: Multiband wavelet age modeling for a ∼293 m (∼600 Kyr) sediment core from chew Bahir Basin, Southern Ethiopian Rift. Front. Earth Sci. **9**(March), 1–15 (2021). https://doi.org/10.3389/feart.2021.594047

Eltijani, A., Molnár, D., Makó, L., Geiger, J., Sümegi, P.: Application of parameterized grain-size end-member modeling in the study of quaternary oxbow lake sedimentation: a case study of tövises bed sediments in the Eastern Great Hungarian Plain. Quaternary **5**(4), 44 (2022a). https://doi.org/10.3390/quat5040044

Eltijani, A., Molnár, D., Makó, L., Geiger, J., Sümegi, P.: Applying grain-size and compositional data analysis for interpretation of the quaternaoxbow lake sedimentation processes: eastern great Hungarian plain. Studia Quaternaria **39**(2), 83–93 (2022b). https://doi.org/10.24425/sq.2022.140885

Eltijani, A., Molnár, D.: Dataset of quaternary abandoned channel in Tövises bed, Great Hungarian Plain. Mendeley Data (2023). https://doi.org/10.17632/fgjgv2ymxp.2

Feldman, R., Sanger, J.: The Text Mining Handbook: Advanced Approaches in Analyzing Unstructured Data. Cambridge University Press, Cambridge (2007)

Flood, R.P., Orford, J.D., McKinley, J.M., Roberson, S.: Effective grain size distribution analysis for interpretation of tidal-deltaic facies: West Bengal Sundarbans. Sed. Geol. **318**, 58–74 (2015). https://doi.org/10.1016/j.sedgeo.2014.12.007

Folk, R.L.: The distinction between grain size and mineral composition in sedimentary-rock nomenclature. J. Geol. **62**(4), 344–359 (1954). https://doi.org/10.1086/626171

Gossel, W., Laehne, R.: Time series analysis with sample applications in geosciences applications of time series analysis in geosciences: an overview of methods and sample applications time series analysis with sample applications in geosciences. Hydrol. Earth Syst. Sci. Discuss **10**, 12793–12827 (2013). https://doi.org/10.5194/hessd-10-12793-2013

Hicks, J.L., Evans, J.E.: Oxbow Lakes as geological archives of historical changes in channel substrate, Swan Creek, Toledo, Ohio (USA). Open J. Modern Hydrol. **12**(02), 32–54 (2022). https://doi.org/10.4236/ojmh.2022.122003

Hiscott, R.N.: Traction-carpet stratification in turbidites—fact or fiction? J. Sediment. Res. A Sediment. Petrol. Processes **64A**(2), 204–208 (1994). https://doi.org/10.1306/d42681ad-2b26-11d7-8648000102c1865d

Hiscott, R.N.: Grading, graded bedding BT. In: Middleton, G.V., Church, M.J., Coniglio, M., Hardie, L.A., Longstaffe, F.J. (eds.) Encyclopedia of sediments and sedimentary rocks, pp. 333–335. Springer, Dordrecht (2003)

Hooke, J.M.: River channel adjustment to meander cutoffs on the river bollin and river dane, Northwest England. Geomorphology **14**(3), 235–253 (1995). https://doi.org/10.1016/0169-555X(95)00110-Q

Ielpi, A., Lapôtre, M.G.A., Finotello, A., Ghinassi, M.: Planform-asymmetry and backwater effects on river-cutoff kinematics and clustering. Earth Surf. Processes Landf. **46**(2), 357–370 (2021). https://doi.org/10.1002/esp.5029

Kadkhodaie, A., Rezaee, R.: Intelligent sequence stratigraphy through a wavelet-based decomposition of well log data. J. Natl. Gas Sci. Eng. **40**, 38–50 (2017). https://doi.org/10.1016/j.jngse.2017.02.010

Katra, I., Yizhaq, H.: Intensity and degree of segregation in bimodal and multimodal grain size distributions. Aeol. Res. **27**, 23–34 (2017). https://doi.org/10.1016/j.aeolia.2017.05.002

Konert, M., Vandenberghe, J.: Comparison of laser grain size with pipette and sieve analysis. Sedimentology **44**(523–535), 523–535 (1997)

Lau, K.M., Weng, H.: Climate signal detection using wavelet transform: how to make a time series sing. Bull. Am. Meteorol. Soc. **76**(12), 2391–2402 (1995). https://doi.org/10.1175/1520-0477(1995)076%3c2391:CSDUWT%3e2.0.CO;2

Li, Z., Sun, Z., Liu, J., Dong, H., Xiong, W., Sun, L., Zhou, H.: Prediction of river sediment transport based on wavelet transform and neural network model. Appl. Sci. (switzerland) **12**, 2 (2022). https://doi.org/10.3390/app12020647

Palazón, L., Navas, A.: Variability in source sediment contributions by applying different statistic test for a pyrenean catchment. J. Environ. Manag. **194**, 42–53 (2017). https://doi.org/10.1016/j.jenvman.2016.07.058

Passega, R.: Grain size representation by CM patterns as a geologic tool. J. Sediment. Res. **34**(4), 830–847 (1964). https://doi.org/10.1306/74d711a4-2b21-11d7-8648000102c1865d

Perez-Muñoz, T., Velasco-Hernandez, J., Hernandez-Martinez, E.: wavelet transform analysis for lithological characteristics identification in siliciclastic oil fields. J. Appl. Geophys. **98**(October), 298–308 (2013). https://doi.org/10.1016/j.jappgeo.2013.09.010

Prokoph, A., Timothy Patterson, R.: Application of wavelet and regression analysis in assessing temporal and geographic climate variability: Eastern Ontario, Canada as a Case Study. Atmosphere Ocean **42**(3), 201–212 (2004). https://doi.org/10.3137/ao.420304

Rivera, N.A., Ray, S., Jensen, J.L., Chan, A.K., Ayers, W.B.: Detection of cyclic patterns using wavelets: an example study in the Ormskirk Sandstone, Irish Sea. Math. Geol. **36**(5), 529–543 (2004). https://doi.org/10.1023/B:MATG.0000037735.34280.42

Roberson, S., Weltje, G.J.: Inter-instrument comparison of particle-size analysers. Sedimentology **61**(4), 1157–1174 (2014). https://doi.org/10.1111/sed.12093

Schwarzacher, W.: Repetitions and cycles in stratigraphy. 51–75 (2000)

Sedláček, J., Kapustová, V., Šimíček, D., Bábek, O., Sekanina, M.: Initial stages and evolution of recently abandoned meanders revealed by multi-proxy methods in the odra river (Czech Republic). Geomorphology **333**, 16–29 (2019). https://doi.org/10.1016/j.geomorph.2019.02.027

Shen, Z., Aeschliman, M., Conway, N.: Paleodischarge reconstruction using oxbow lake sediments complicated by shifting hydrological connectivity. Quatern. Int. (2021). https://doi.org/10.1016/j.quaint.2021.07.004

Sun, D., Bloemendal, J., Rea, D.K., Vandenberghe, J., Jiang, F., An, Z., Ruixia, Su.: Grain-size distribution function of polymodal sediments in hydraulic and Aeolian environments, and numerical partitioning of the sedimentary components. Sed. Geol. **152**(3–4), 263–277 (2002). https://doi.org/10.1016/S0037-0738(02)00082-9

Szilágyi, S.S., Geiger, J.: Sedimentological study of the Szőreg-1 Reservoir (Algyő Field, Hungary): a combination of traditional and 3D sedimentological approaches. Geologia Croatica **65**(1), 77–90 (2012). https://doi.org/10.4154/GC.2012.06

Tarar, Z.R., Ahmad, S.R., Ahmad, I., Majid, Z.: Detection of sediment trends using wavelet transforms in the Upper Indus River. Water (switzerland) **10**(7), 1–17 (2018). https://doi.org/10.3390/w10070918

Toonen, W.H.J., Kleinhans, M.G., Cohen, K.M.: Sedimentary architecture of abandoned channel fills. Earth Surf. Proc. Land. **37**(4), 459–472 (2012). https://doi.org/10.1002/esp.3189

Ward, J.H.: Hierarchical grouping to optimize an objective function. J Am Stat Assoc **58**(301), 236–244 (1963)

Wentworth, C.K.: A scale of grade and class terms for clastic sediments. J. Geol. **30**(5), 377–392 (1922)

Wren, D.G., Taylor, J.M., Rigby, J.R., Locke, M.A., Yasarer, L.M.W.: Short term sediment accumulation rates reveal seasonal time lags between sediment delivery and deposition in an Oxbow Lake. Agr. Ecosyst. Environ. **281**(May), 92–99 (2019). https://doi.org/10.1016/j.agee.2019.05.007